Cell, Vol. 102, 175–187, July 21, 2000, Copyright ©2000 by Cell Press

Genetic Evidence for Selective Transport of Opsin and Arrestin by Kinesin-II in Mammalian Photoreceptors

Joseph R. Marszalek,*†‡ Xinran Liu,† Elizabeth A. Roberts,*†‡ Daniel Chui,*‡ Jamey D. Marth,*‡ David S. Williams,† and Lawrence S. B. Goldstein*†‡§

*Department of Cellular and Molecular Medicine
†Department of Pharmacology
‡Howard Hughes Medical Institute
University of California, San Diego
9500 Gilman Drive
La Jolla, California 92093

Summary

To test whether kinesin-II is important for transport in the mammalian photoreceptor cilium, and to identify its potential cargoes, we used Cre-loxP mutagenesis to remove the kinesin-II subunit, KIF3A, specifically from photoreceptors. Complete loss of KIF3A caused large accumulations of opsin, arrestin, and membranes within the photoreceptor inner segment, while the localization of α-transducin was unaffected. Other membrane, organelle, and transport markers, as well as opsin processing appeared normal. Loss of KIF3A ultimately caused apoptotic photoreceptor cell death similar to a known opsin transport mutant. The data suggest that kinesin-II is required to transport opsin and arrestin from the inner to the outer segment and that blocks in this transport pathway lead to photoreceptor cell death as found in retinitis pigmentosa.

Introduction

Many specialized cells require large volumes of intracellular transport because of their large size, or idiosyncratic geometry. Vertebrate photoreceptors, in particular, have a substantial transport burden owing to their unique organization. These cells have most of their biosynthetic machinery located in the photoreceptor cell body and inner segment, but the construction of the phototransducing outer segment disks takes place in the photoreceptor outer segment, which is located on the other side of a narrow connecting cilium. How materials needed for phototransduction, such as opsin, arrestin, and transducin, are moved to the outer segment, remains unknown. It has been suggested that motor proteins, including kinesin-II, may drive the necessary transport processes.

The kinesin-II holoenzyme was first identified in sea urchin (Cole et al., 1993), and subsequently in most species and found to be composed of two motor subunits and one nonmotor accessory subunit (for review see Marszalek and Goldstein, 2000). Genetic and localization experiments in *Chlamydomonas*, *Tetrahymena thermophila*, *C. elegans*, and mouse, and microinjection experiments in sea urchin support the proposal that kinesin-II is essential for the construction and maintenance of morphologically typical varieties of motile and nonmotile cilia and flagella (for review see Marszalek and Goldstein, 2000). While there is evidence that members of the kinesin-II family may transport choline acetyltransferase in *Drosophila* axons (Ray et al., 1999) and fodrin in mammalian axons (Takeda et al., 2000), the cargoes moved by kinesin-II in cilia and flagella are not yet identified. In *Chlamydomonas,* kinesin-II appears to transport a large protein complex, termed a raft, possibly with protein cargoes attached, from the sites of synthesis in the cell body to the sites of utilization at the tip of the flagellum (Kozminski et al., 1995; Piperno and Mead, 1997; Cole et al., 1998). It remains unknown, however, whether the highly modified and atypical connecting cilium that links the photoreceptor inner and outer segments utilizes kinesin-II for transport within the connecting cilium. Support for the proposition that kinesin-II performs important transport functions in photoreceptors comes from the observation that the KIF3A motor subunit of kinesin-II localizes to the connecting cilium of photoreceptor cells in a variety of species (Beech et al., 1996; Muresan et al., 1997; Whitehead et al., 1999). However, there is no functional evidence that KIF3A (kinesin-II) is required for transport in photoreceptors.

To address directly the issues of kinesin-II cargoes and function in photoreceptor cells, we used a genetic approach to test whether KIF3A is essential for photoreceptor survival and transport within murine photoreceptor cells. Since systemic deletion of KIF3A results in embryonic lethality (Marszalek et al., 1999; Takeda et al., 1999), we utilized Cre-loxP conditional mutagenesis to eliminate KIF3A protein only from photoreceptors in 3-week-old postnatal mice. Complete loss of KIF3A resulted in aberrant opsin and arrestin transport, accumulation of proteinaceous and membranous material within the inner segment of photoreceptors, and subsequent photoreceptor death via the apoptotic cell death pathway. These data establish that KIF3A is essential for photoreceptor survival and support the hypothesis that KIF3A transports opsin, arrestin, and possibly other material from the photoreceptor inner to outer segment through the connecting cilium.

Results

Generation of Mice Lacking KIF3A Only in Photoreceptors

To determine the function of KIF3A in photoreceptors, we used Cre-loxP mutagenesis to generate mice that have the *KIF3A* gene deleted only in photoreceptor cells. A KIF3A conditional mutant allele ($KIF3A^{flox}$) was generated that is identical to the wild-type KIF3A allele ($KIF3A^{WT}$), except that it has two loxP site–specific recombination sequences inserted into the intronic DNA sequences that flank the second protein coding exon (Marszalek et al., 1999) (Figure 1A). Since only intronic sequences of the *KIF3A* gene were altered, the $KIF3A^{flox}$ allele should produce the normal amount and quality of KIF3A protein. When we examined the neuroretina and brain from $KIF3A^{WT}/KIF3A^{WT}$ and $KIF3A^{flox}/KIF3A^{flox}$ animals by Western immunoblotting, we found no alteration in the size or amount of KIF3A protein, establishing that

§To whom correspondence should be addressed (e-mail: lgoldstein@ucsd.edu).

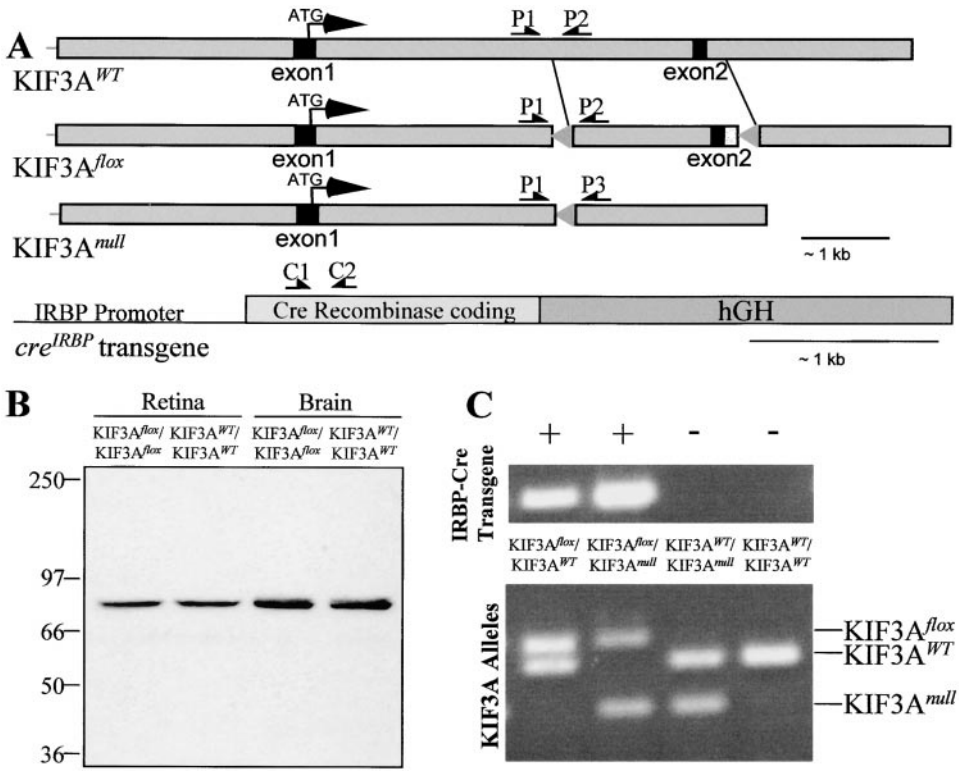

Figure 1. Generation and Characterization of New KIF3A Alleles and *cre*^{IRBP} Transgene

(A) LoxP sites were introduced into intronic sequence that flank the second protein coding exon to generate the KIF3A^{flox} allele. Removing the DNA between the loxP sites produced the KIF3A^{null} allele. Location of the PCR primers used to identify the KIF3A alleles are labeled. The *cre*^{IRBP} transgene construct and the location of the primers that were used to score for the presence or absence of the transgene in mice are pictured at the bottom.

(B) Western immunoblot probe for KIF3A protein in 10 μg of total retina and brain extract from KIF3A^{flox}/KIF3A^{flox} and KIF3A^{WT}/KIF3A^{WT} using anti-KIF3A antibody (Marszalek et al., 1999).

(C) Ethidium bromide–stained gels showing the presence or absence of the *cre*^{IRBP} transgene in mouse tail DNA (upper panel) and which KIF3A alleles are present (lower panel).

the KIF3A^{flox} allele and the KIF3A^{WT} allele are interchangeable (Figure 1B). Therefore, in mice that do not contain the *cre*^{IRBP} transgene, the KIF3A^{WT} and KIF3A^{flox} alleles were used interchangeably.

The photoreceptor-specific IRBP (*I*nterphotoreceptor matrix *R*etinoid *B*inding *P*rotein) promoter was used to direct the expression of the Cre recombinase protein in photoreceptor cells (Figure 1A, bottom). The IRBP promoter has been extensively characterized and found to drive expression of reporter genes primarily in photoreceptor cells (most recently Bobola et al., 1995). Animals possessing the KIF3A^{flox} allele and the *cre*^{IRBP} transgene convert the KIF3A^{flox} allele to a KIF3A^{null} allele only in photoreceptor cells because the Cre recombinase is only expressed in these cells. Excision of the second protein coding exon results in a frameshift of the normal KIF3A coding sequence thereby producing a 62 amino acid protein that only shares the original methionine with the wild-type KIF3A protein.

To determine the timing and quantity of conversion of the KIF3A^{flox} allele to the KIF3A^{null} allele that is catalyzed by the *cre*^{IRBP} transgene in photoreceptor cells, we performed competitive quantitative PCR on DNA that was isolated from the neuroretinas of KIF3A^{flox}/KIF3A^{WT}; *cre*^{IRBP} animals at various ages. The extent of recombination within each neuroretina was determined by quantifying the intensity of the KIF3A^{null} and KIF3A^{flox} bands and then calculating the percentage of KIF3A^{null} allele present in the unknown samples by comparison to a standard composed of various mixtures of DNAs isolated from the neuroretinas of KIF3A^{flox}/KIF3A^{WT} and KIF3A^{WT}/KIF3A^{null} animals (Figures 2A and 2B; see Experimental Procedures). Since the KIF3A^{WT} allele does not undergo recombination, it was not quantified and excluded from the calculation. We selected the KIF3A^{flox}/KIF3A^{WT}; *cre*^{IRBP} for recombination analysis instead of the KIF3A^{flox}/KIF3A^{null}; *cre*^{IRBP} or KIF3A^{flox}/KIF3A^{flox}; *cre*^{IRBP} genotypes for two important reasons. First, if loss of KIF3A protein results in rapid cell death, the amount of excision will be substantially underestimated in the KIF3A^{flox}/KIF3A^{null}; *cre*^{IRBP} and KIF3A^{flox}/KIF3A^{flox}; *cre*^{IRBP} retinas because only the remaining KIF3A heterozygous and wild-type cells will be scored. Second, it is possible to detect accurately low levels of recombination in KIF3A^{flox}/KIF3A^{WT}; *cre*^{IRBP} animals because there is no background KIF3A^{null} allele present in KIF3A^{flox}/KIF3A^{WT}; *cre*^{IRBP} animals.

Since only 70% of the cells within the neuroretina are photoreceptor cells (Jeon et al., 1998), we expected that no more than 70% of the KIF3A^{flox} allele could be converted to the KIF3A^{null} allele in the retinas of KIF3A^{flox}/KIF3A^{WT}; *cre*^{IRBP} animals. We found significant variation in the amount of recombination among animals at every age examined (Figure 2C), except at 2 weeks of age and

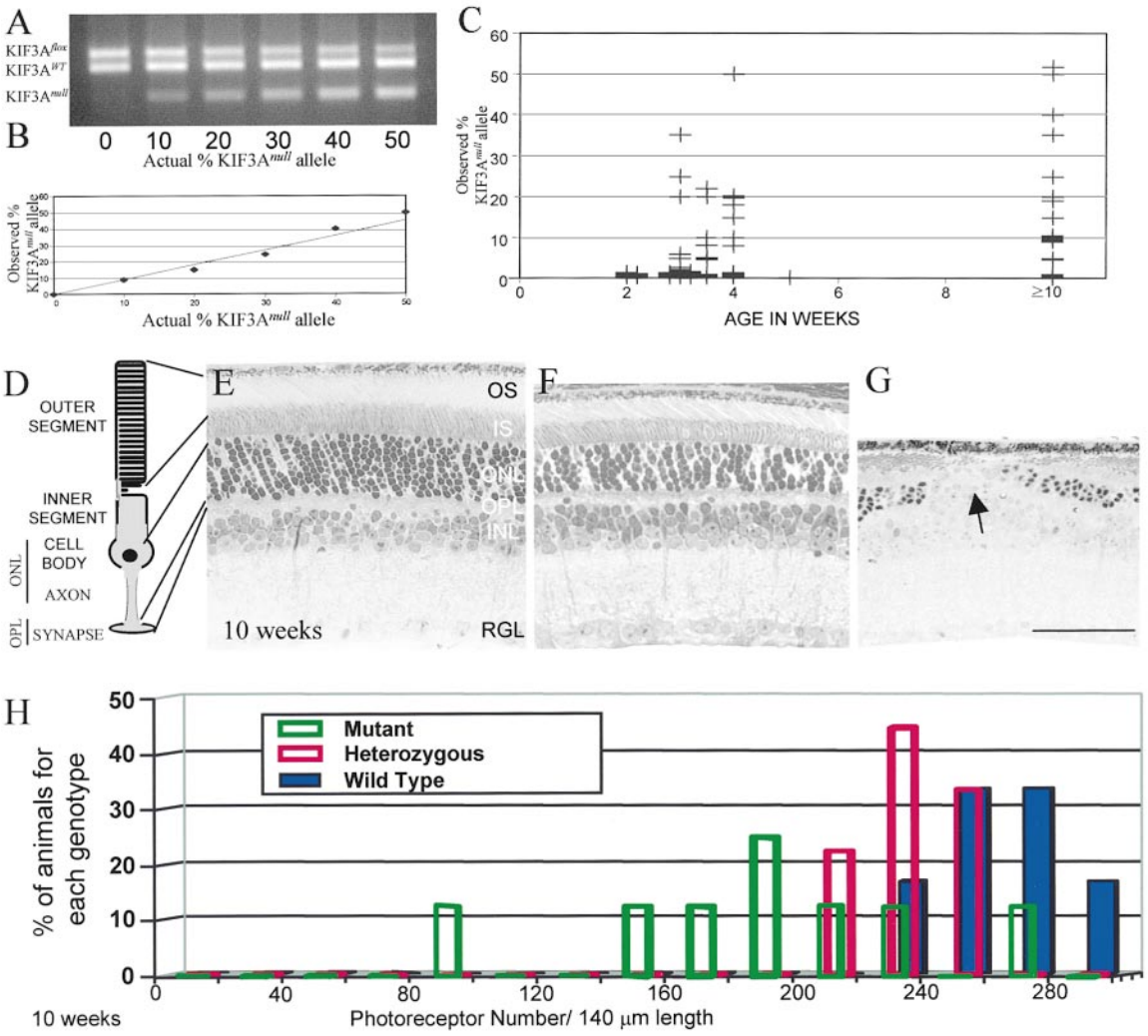

Figure 2. Variation in Extent of Recombination with the *cre*^{IRBP} Transgene

(A) Ethidium bromide–stained gel of a dilution series of various mixtures of KIF3A^{null}/KIF3A^{WT} and KIF3A^{flox}/KIF3A^{WT} neuroretina DNA. (B) Graph comparing the actual percentage of KIF3A^{null} allele in each mixture to that calculated from the KIF3A^{null} and KIF3A^{flox} band intensities of the ethidium bromide–stained gel in (A). Note the linearity of the dilution series. (C) Graph showing the percentage of KIF3A^{null} allele observed in the retinas of KIF3A^{flox}/KIF3A^{WT}; *cre*^{IRBP} animals at various ages. (2 weeks, n = 11; 3 weeks, n = 28; 3.5 weeks, n = 10; 4 weeks, n = 15; 10–30 weeks, n = 26). (D) Cartoon of a photoreceptor that depicts the different regions of a photoreceptor cell. (E–G) Light microscopy images of retinas from 10-week-old animals. (E) A normal retina from a KIF3A^{WT}/KIF3A^{WT} animal. (F) A moderately affected retina from a KIF3A^{flox}/KIF3A^{null}; *cre*^{IRBP} animal. (G) A severely affected retina from a KIF3A^{flox}/KIF3A^{null}; *cre*^{IRBP} animal. The light staining of INL nuclei in (G) is due to this retina being embedded in LR White, while (E) and (F) are in epon. Also note the decrease in the number of photoreceptor nuclei and the decrease in the length of inner and outer segments in (E) and (F). (H) Graph showing the distribution of photoreceptor cell number among 10-week-old animals. (KIF3A Wild Type, n = 6; KIF3A Heterozygous, n = 13; KIF3A Null, n = 8). Note the broad distribution of cell number among mutants and that more than 50% of the mutant animals have less photoreceptor nuclei than the lowest control animals. OS, outer segment; IS, inner segment; ONL, outer nuclear layer; OPL, outer plexiform layer; INL, inner nuclear layer; RGL, retinal ganglion layer. Scale bar = 50 μm.

earlier when no excision was detected. Additionally, in any single animal, the amount of recombination was identical in each eye (data not shown). At 3 weeks of age and older, the amount of recombination among animals varied from none to nearly all of the KIF3A^{flox} allele converted to the KIF3A^{null} allele in photoreceptor cells (Figure 2C). Most of the excision appears to occur between 3 and 4 weeks of age, since the percentage of animals that exhibit >5% recombination increases from 18% at 3 weeks to 53% at 4 weeks of age. However, additional recombination at the KIF3A^{flox} allele appears to be minimal after 4 weeks of age, because the rate of recombination among animals is not statistically different between animals that are 4 and 10-plus weeks of age (t test, p = 0.30), but is significant between animals that are 3 and 10-plus weeks of age (t test, p = 0.001). The cause of the variation in the amount of recombination is unclear, but most likely is due to differences in the genetic backgrounds among mice or inherent variability in *cre*^{IRBP} transgene expression.

Loss of KIF3A Results in Photoreceptor Death

To determine whether the KIF3A protein is important for transport within photoreceptors, we generated KIF3A^{flox}/KIF3A^{null}; *cre*^{IRBP} animals. We used this combination of

alleles, rather than two KIF3A^{flox} alleles to simplify analysis because all of the photoreceptors in these animals will be one of two genotypes: either KIF3A^{flox}/KIF3A^{null} or KIF3A^{null}/KIF3A^{null}. Examination of 10-week-old KIF3A^{flox}/KIF3A^{null}; *cre*^{IRBP} retinas by light microscopy revealed that the number of photoreceptor nuclei in these animals is variable, ranging from no detectable reduction to loss of 80% of the photoreceptors (Figures 2E–2H). In the retina that had lost 80% of its photoreceptor cells, there were some regions completely devoid of all photoreceptor nuclei (Figure 2G, arrow). However, in all of the less severely affected retinas, the loss of photoreceptors appeared homogenous throughout the retina and both retinas of a single animal displayed the same degree of photoreceptor cell loss (Figure 2F). No cell loss was observed in 2-week-old KIF3A^{flox}/KIF3A^{null}; *cre*^{IRBP} retinas indicating that the reduced photoreceptor cell number we observe is due to photoreceptor cell loss and not lack of cell generation (data not shown). Additionally, no effect of the *cre*^{IRBP} allele alone was observed (data not shown).

To determine whether retinal defects were restricted to photoreceptor cells, we performed a morphological and quantitative examination of the various cellular layers of the retinas from 10-week-old KIF3A^{flox}/KIF3A^{null}; *cre*^{IRBP} animals that exhibited moderate to severe photoreceptor cell loss. We observed no obvious differences in cell morphology or quantity in the retinal ganglion or inner nuclear layer between KIF3A^{flox}/KIF3A^{null}; *cre*^{IRBP} animals and KIF3A^{WT}/KIF3A^{WT} or KIF3A^{flox} /KIF3A^{WT} controls (data not shown). We conclude that the retinal defects in KIF3A^{flox}/KIF3A^{null}; *cre*^{IRBP} animals are restricted to photoreceptor cells within the retina and are due to Cre mediated recombination with deletion of the *KIF3A* gene.

Accumulation of Material in the Inner Segment of KIF3A Mutant Photoreceptors

To identify abnormalities that could provide insight into the defects resulting from removal of KIF3A protein, we examined the retinas from KIF3A^{flox}/KIF3A^{null}; *cre*^{IRBP} animals at various ages by electron microscopy. If KIF3A is responsible for transport of material from the inner segment to the outer segment along the connecting cilium, we expected accumulation of material within the inner segment once KIF3A protein was removed. Consistent with this hypothesis, we observed striking accumulation of vesicular and proteinaceous material in the inner segment of photoreceptors only in KIF3A^{flox}/KIF3A^{null}; *cre*^{IRBP} animals that were between 21 and 28 days of age (Figures 3A and 3B). In the most severely affected photoreceptors, accumulations were enormous, often larger in diameter than the normal inner segment (Figures 3A and 3B).

To determine if the localization defect we observed was a consequence of a defective connecting cilium, we cut serial cross-sections of photoreceptors to examine the integrity of the connecting cilium in cells with inner segment accumulations. Examination of these sections revealed no obvious structural defect of the connecting cilium in cells that possessed inner segment accumulations (data not shown).

We also performed immuno-EM for opsin and peripherin, two proteins that normally localize to the outer segment, to determine if either of these proteins localized within the inner segment accumulations. This analysis revealed that while opsin was present around the periphery of the accumulation, it was not present within the accumulation (Figure 3B). We did not observe any obvious accumulation of peripherin within or around any accumulations (data not shown). Accumulation of material within the inner segment of photoreceptors from KIF3A heterozygous or wild-type control retinas was never observed indicating that the accumulations were linked to deletion of the *KIF3A* gene and most likely a result of the loss of the majority, if not all, of the KIF3A protein. Additionally, in KIF3A^{flox}/KIF3A^{null}; *cre*^{IRBP} animals older than 4 weeks of age, we did not observe any accumulation of material in the inner segment of any photoreceptors, nor many cells that were in the process of degeneration, suggesting that the majority of cell death occurred by 4 weeks of age. In many KIF3A^{flox}/KIF3A^{null}; *cre*^{IRBP} animals, we observed photoreceptor cells that had degenerated to opsin-containing fragments (Figure 3C). These profiles bear a striking resemblance to those described as a final stage of photoreceptor degeneration in transgenic mice expressing P347S opsin, which is not targeted properly to the outer segment (Li et al., 1996).

Opsin Mislocalization Precedes Photoreceptor Cell Death

To determine whether photoreceptor cell death caused by loss of KIF3A is a consequence of defective transport of material from the inner to the outer segment, we used immunofluorescence and electron microscopy (EM) analysis to examine the neuroretinas of KIF3A^{flox}/KIF3A^{null}; *cre*^{IRBP} animals at various ages. Opsin is the most heavily trafficked cargo to the outer segment and defects in its transport have been implicated as a cause of photoreceptor degeneration and retinitis pigmentosa (Roof et al., 1994; Sung et al., 1994; Colley et al., 1995; Li et al., 1996). Opsin accumulation is normally restricted primarily to the outer segment of photoreceptor cells (Figure 3B, cells with asterisk, and 4A). However, the first defect that we observed by immuno-EM (Figure 3D, arrows) and IF (Figure 4B, arrowheads) in a subset of KIF3A^{flox}/KIF3A^{null}; *cre*^{IRBP} retinas is accumulation of opsin within the cytoplasm of the inner segment, but not on the plasma membrane, around 21–24 days of age. At this first stage, we do not detect any obvious photoreceptor cell death or morphological abnormalities by conventional EM or light microscopy.

At 24–28 days of age, a subset of KIF3A^{flox}/KIF3A^{null}; *cre*^{IRBP} animals (8 out of 29, 28%) exhibit abnormal accumulation of opsin in the cytoplasm and plasma membrane throughout the cell (Figures 4B and 4C). Many photoreceptors possessed obvious opsin accumulation within the inner segment, and weak opsin staining within the cell body (Figure 4B, arrow). In retinas where opsin staining was generally stronger in the inner segment than the cell body of most cells, we did not observe significant cell loss (Figure 4B). However, at apparently later stages, when strong opsin signal was detected within the cell body, synaptic and inner segment regions of the photoreceptor cells (Figure 4C), photoreceptor cell loss was observed. Consistent with the variable recombination observed by PCR and variable photoreceptor cell loss, the number of cells displaying defective opsin localization varied among animals from none to as many as 75% of the remaining cells being affected.

To determine whether null photoreceptor cells were dying through an apoptotic mechanism, we performed

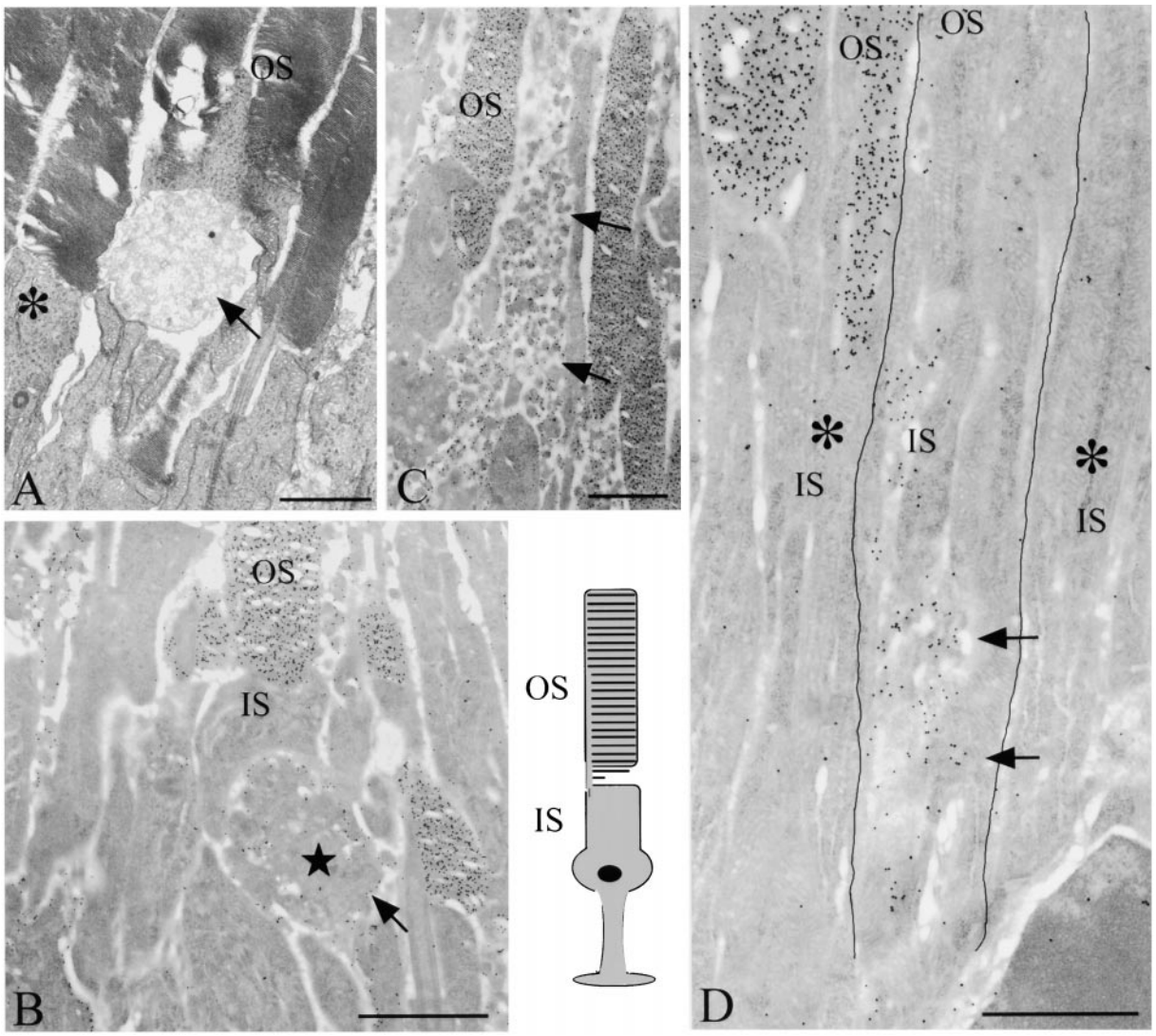

Figure 3. Ultrastructural Abnormalities Observed in Photoreceptors from KIF3A^{flox}/KIF3A^{null}; *cre*^{IRBP} Retinas

(A–D) Retina from a KIF3A^{flox}/KIF3A^{null}; *cre*^{IRBP} animal. (A) EM micrograph of a proteinaceous accumulation of material in the inner segment of a mutant photoreceptor cell (arrow). Note the normal inner segment in the cell that is on the right of the mutant cell (asterisks). (B) Immunogold labeling of a proteinaceous accumulation for opsin (arrow). Note the minimal labeling within the accumulation (star). (C) Immunogold labeling of a cell whose outer segment has undergone fragmentation (arrows). (D) Immunogold labeling of photoreceptor cells for opsin. Note the gold particles in the inner segment of a mutant photoreceptor cell (arrows) that is surrounded by normal cells that do not show opsin signal (asterisks). The black lines outline the inner segment of a mutant cell. OS, outer segment; IS, inner segment. Scale bar = 1 μm.

TUNEL assays on all of the mutant neuroretinas that displayed aberrant opsin accumulation. TUNEL positive nuclei were detected primarily in retinas that displayed strong staining of opsin throughout the photoreceptor cells (Figure 4E). Most opsin positive cells were not TUNEL positive (Figure 4E, arrowhead), while almost 90% of TUNEL positive cells exhibited significant misaccumulation of opsin (Figure 4E, open arrowhead). The occasional TUNEL positive nuclei that do not exhibit opsin misaccumulation (Figure 4E, arrow) may be KIF3A^{flox}/KIF3A^{null} cells that did not undergo Cre-mediated recombination, and are dying as a result of degenerating neighboring KIF3A null cells, similar to that observed in P347S mutant opsin/wild-type chimeric retinas (Huang et al., 1993). Thus, it is likely that opsin misaccumulation precedes the entrance of the cell into the apoptotic cell death pathway. Therefore, mislocalization of opsin may precede and cause the activation of the apoptosis cell death pathway in mutant photoreceptors. Initiation of the apoptotic cell death pathway has also been reported in opsin, β-phosphodiesterase (*rd*) and peripherin (*rds*) mutant mice and seems to be a common final step to cell death in photoreceptor mutants (Chang et al., 1993).

Most Photoreceptor Transport Pathways Are Normal after Loss of KIF3A

To determine whether the opsin localization defect we observed in mutant photoreceptor cells resulted from general disruption of intracellular transport, we used double-staining immunofluorescence to examine the distribution of other integral membrane proteins that are

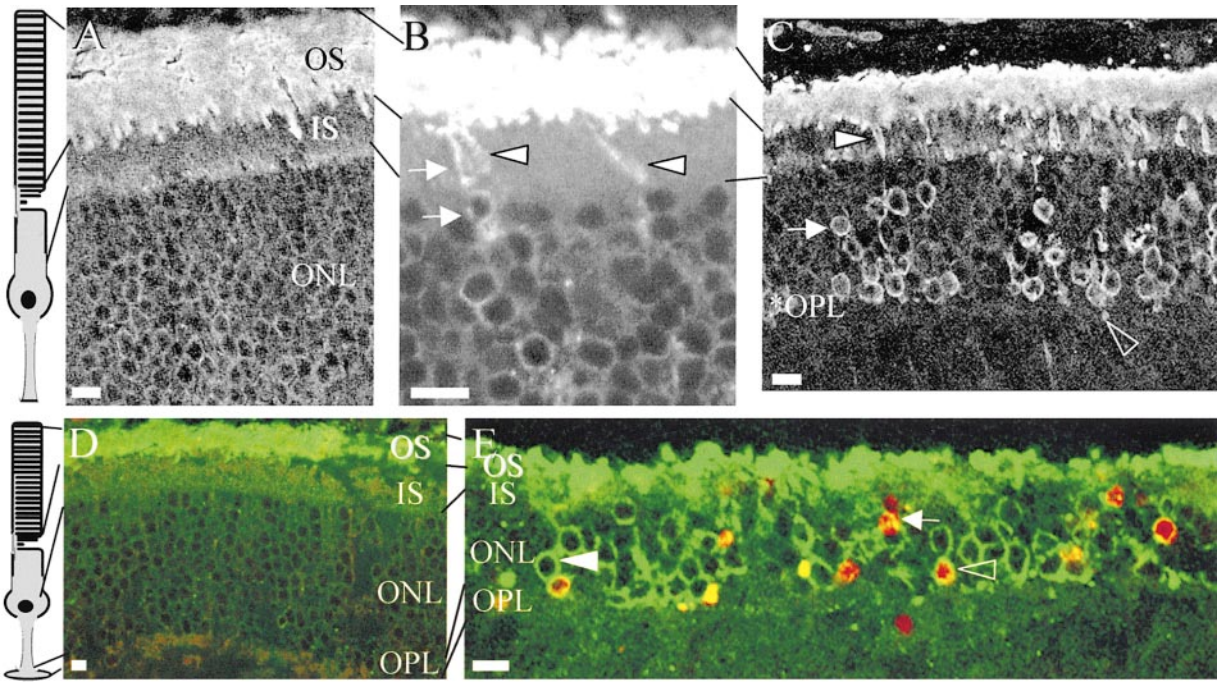

Figure 4. Misaccumulation of Opsin and Apoptotic Photoreceptor Cell Death in KIF3A^{flox}/KIF3A^{null}; *cre*^{IRBP} Animals

(A–C) Immunofluorescent staining for opsin. (A) A retina from a KIF3A^{WT}/KIF3A^{WT} animal. (B) A moderately affected retina from a KIF3A^{flox}/KIF3A^{null}; *cre*^{IRBP} animal. (C) A severely affected retina from a KIF3A^{flox}/KIF3A^{null}; *cre*^{IRBP} animal. Note the accumulation of opsin in some inner segments (arrowhead), cell bodies (arrows), and synapse (open arrowhead) in (C). The asterisk denotes the OPL. (D and E) Double labeling for opsin (green) and TUNEL positive cells (red). (D) A KIF3A^{WT}/KIF3A^{WT} retina. (E) A retina from a KIF3A^{flox}/KIF3A^{null}; *cre*^{IRBP} animal. Note that most cells that are TUNEL positive exhibit aberrant opsin localization (open arrowhead), but most cells that misaccumulate opsin are not TUNEL positive (arrowhead). A rare TUNEL positive, opsin negative cell is noted with an arrow. OS, outer segment; IS, inner segment; ONL, outer nuclear layer. Scale bar = 5 μm.

trafficked to the synapse (SV2, synaptotagmin, VAMP, and SNAP-25) or outer segment (peripherin) and cytosolic proteins normally localized to the outer segment (α-transducin and arrestin). We never observed aberrant localization of any of the synaptic cargoes in any of the photoreceptors with aberrant opsin accumulation (Figures 5B–5D and data not shown), indicating that the transport of membranous cargoes to the synapse is not substantially disrupted within mutant photoreceptor cells.

Examination of arrestin (a cytosolic outer segment protein) in mutant retinas revealed that in all of the inner segments of cells with mislocalized opsin, some arrestin colocalized with the opsin signal (Figures 5F–5H, arrowheads). Peripherin localization, on the other hand, was not significantly altered in many mutant photoreceptor cells (Figures 5J–5L, green arrowheads), especially in the modestly affected retinas. However, in the most severely affected mutant retinas (n = 3), many of the mutant photoreceptor cells that exhibited aberrant opsin localization also exhibited peripherin mislocalization, (Figures 5J–5L, red arrowheads). Taken together, these data suggest that opsin misaccumulation occurred before peripherin misaccumulation. Additionally, within a single mutant photoreceptor, misaccumulated peripherin staining rarely colocalized with opsin (Figure 5L, red arrowheads). Finally, we never observed any misaccumulation of α-transducin in any mutant photoreceptor cells, suggesting that its transport is unaffected by the loss of KIF3A (Figures 5N–5P, arrowheads).

To determine whether severe alterations in the distribution or localization of any of these inner segment organelles might be responsible for, or correlate with aberrant opsin distribution, we examined the endoplasmic reticulum (ER), Golgi apparatus, and mitochondria by immunofluorescence. Double staining experiments with opsin and either COX I—(mitochondria) (Figures 6A–6D), calreticulin—(ER) (Figures 6E–6H), or giantin—(Golgi apparatus) (Figures 6I–6L, arrowheads) revealed that in cells with inner segment opsin accumulation, the distribution of all of these organelles appeared normal (Figure 6) when compared to control retinas.

To determine whether glycosylation still occurred in mutant photoreceptors, we stained mutant neuroretinas with the lectin concanavalin A (Con A), which is specific for mannose residues found on N-glycans produced after entry into the ER and Golgi. We observed significant colocalization of opsin and Con A (Figures 6M–6P, arrowheads) staining especially in the inner segment of mutant photoreceptors, suggesting that aberrantly localized opsin was nonetheless processed through the endoplasmic reticulum and the Golgi apparatus in mutant photoreceptor cells.

Discussion

Photoreceptor Abnormalities in KIF3A Mutant Mice

We examined the consequence of removing the KIF3A motor subunit of kinesin-II from photoreceptor cells using cre-loxP conditional mutagenesis (Marth, 1996). We found that conversion of the KIF3A^{flox} allele to the KIF3A^{null} allele by the *cre*^{IRBP} transgene was variable among

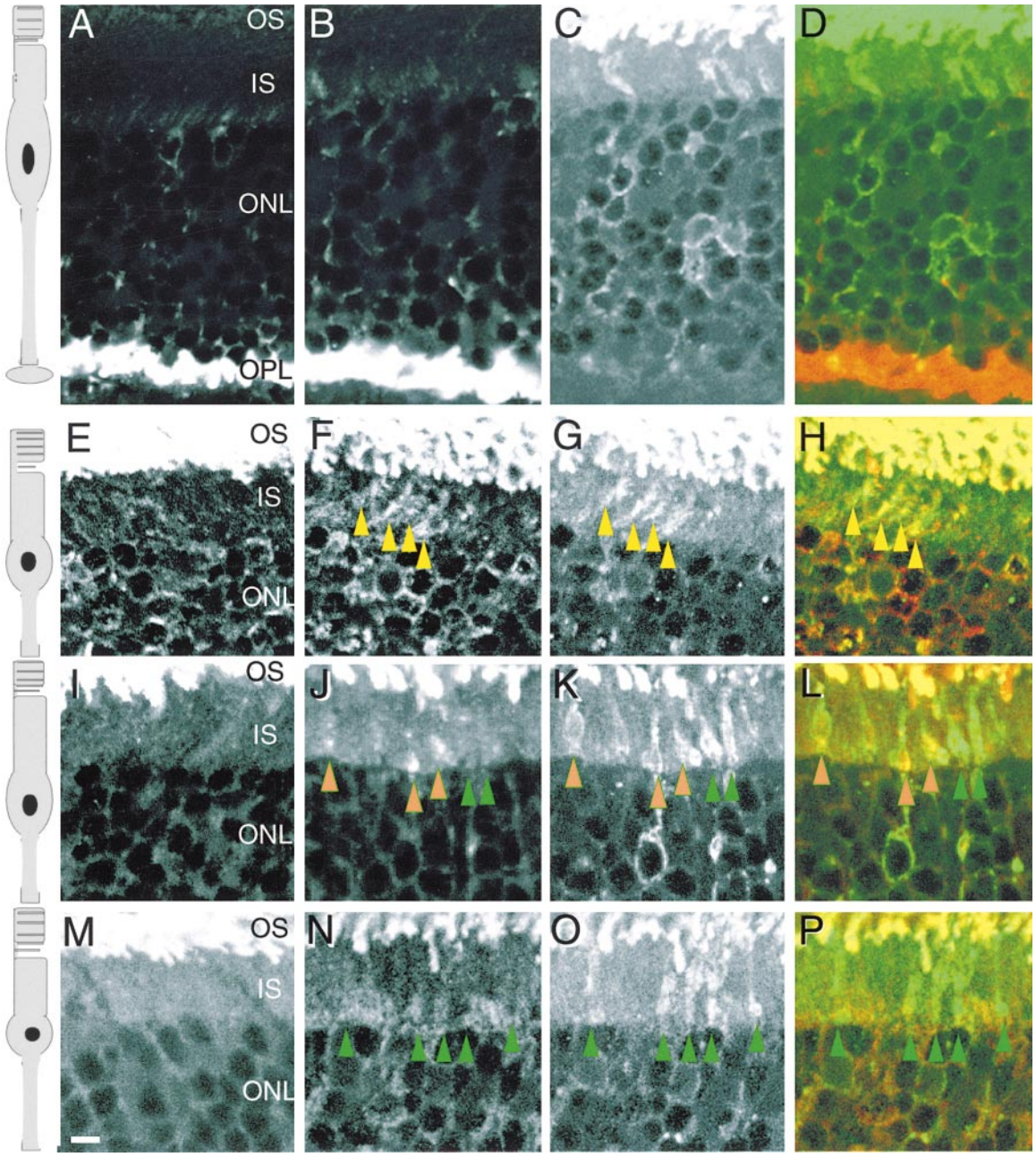

Figure 5. Selective Disruption of Transport in Mutant Photoreceptors

(A) Immunofluorescence of a KIF3A^{WT}/KIF3A^{WT} retina stained for the synaptic protein SV2. (B–D) A retina from a KIF3A^{flox}/KIF3A^{null}; *cre*^{IRBP} animal. (B) Stained for SV2. (C) Stained for opsin. (D) Merge of B (red) and C (green). Note that the SV2 signal is limited to the synaptic region. (E) A KIF3A^{WT}/KIF3A^{WT} retina stained for the cytosolic protein arrestin. (F–H) A retina from a KIF3A^{flox}/KIF3A^{null}; *cre*^{IRBP} animal. (F) Arrestin. (G) Opsin. (H) Merge of (F) (red) and (G) (green). (I) A KIF3A^{WT}/KIF3A^{WT} retina stained for the outer segment protein peripherin. (J–L) A retina from a KIF3A^{flox}/KIF3A^{null}; *cre*^{IRBP} animal. (J) Peripherin. (K) Opsin. (L) Merge of (J) (red) and (K) (green). Some inner segments accumulate only opsin (green arrowheads), while others also have some misaccumulated peripherin (red arrowheads). (M) A KIF3A^{WT}/KIF3A^{WT} retina stained for the membrane associated protein α-transducin. (N–P) A retina from a KIF3A^{flox}/KIF3A^{null}; *cre*^{IRBP} animal. (N) Stained for α-transducin. (O) Stained for opsin. (P) Merge of (N) (red) and (O) (green). OS, outer segment; IS, inner segment; ONL, outer nuclear layer; OPL, outer plexiform layer. Scale bar = 5 μm.

animals and did not begin until approximately 3 weeks of age postnatally when photoreceptor outer segments are mature. Disruption of both *KIF3A* genes in photoreceptor cells resulted in defective opsin and arrestin localization, accumulation of unknown material within the inner segment, and rapid photoreceptor cell death, most likely through an apoptotic cell death mechanism.

Kinesin-II Is Required for the Transport of Opsin and Arrestin from the Inner to the Outer Segment

In photoreceptor cells, the minus ends of all of the inner segment microtubules are oriented toward the basal body, which is located in the distal portion of the inner segment, just below the outer segment (Figure 7) (Troutt

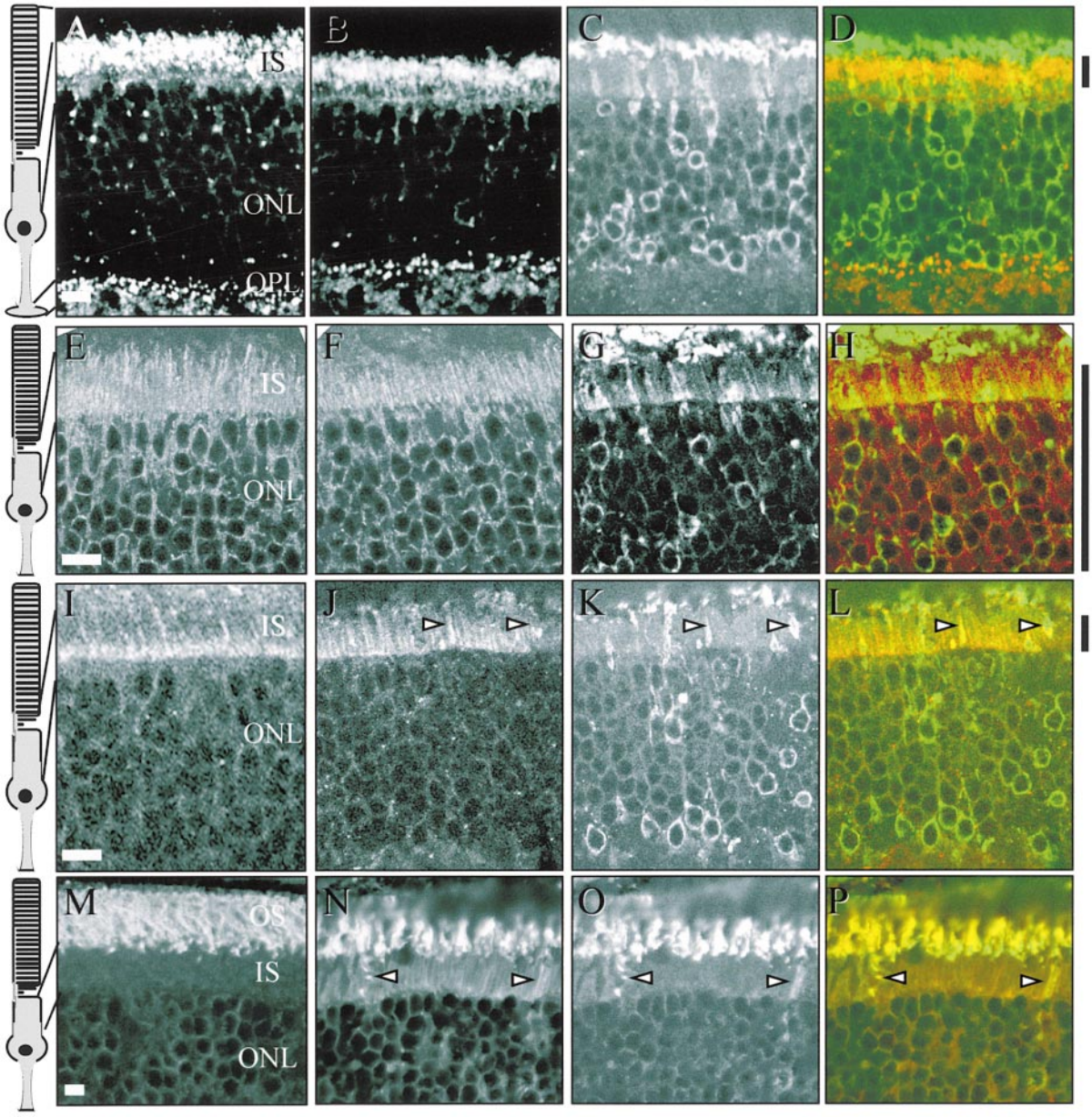

Figure 6. Organelles and Opsin Processing Are Not Altered in Mutant Photoreceptors

(A) A retina from a KIF3A^{WT}/KIF3A^{WT} animal stained for Cox I (mitochondria). Mitochondria are concentrated in the distal portion of the inner segment (black line at right of (D). (B–D) A retina from a KIF3A^{flox}/KIF3A^{null}; *cre*^{IRBP} animal. (B) Stained for Cox I. (C) Stained for opsin. (D) Merge of (B) (red) and (C) (green). (E) A retina from a KIF3A^{WT}/KIF3A^{WT} animal stained for calreticulin (endoplasmic reticulin). The ER is normally found throughout the inner segment and cell body (black line at right of H). (F–H) A retina from a KIF3A^{flox}/KIF3A^{null}; *cre*^{IRBP} animal. (F) Stained for calreticulin. (G) Stained for opsin. (H) Merge of (F) (red) and (G) (green). (I) A retina from a KIF3A^{WT}/KIF3A^{WT} animal stained for giantin (Golgi apparatus). The Golgi apparatus is normally concentrated in the proximal portion of the inner segment (black line at right of L). (J–L) A retina from a KIF3A^{flox}/KIF3A^{null}; *cre*^{IRBP} animal. (J) Stained for giantin. (K) Stained for opsin. (L) Merge of (K) (red) and (L) (green). Note the similarity in the distribution of Cox I, calreticulin and giantin staining between KIF3A^{WT}/KIF3A^{WT} and KIF3A^{flox}/KIF3A^{null}; *cre*^{IRBP} retinas. Also note that none of the organelles examined undergo obvious redistribution within the mutant photoreceptor cells (i.e., no redistribution to the cell body). (M) A retina from a KIF3A^{WT}/KIF3A^{WT} animal stained with the lectin Concanavalin A (glycosylated opsin). (N–P) A retina from a KIF3A^{flox}/KIF3A^{null}; *cre*^{IRBP} animal. (N) Stained with the lectin Concanavalin A. (O) Stained for opsin. (P) Merge of (N) (red) and (O) (green). OS, outer segment; IS, inner segment; ONL, outer nuclear layer. Scale bar = 5 μm.

and Burnside, 1988). Therefore, transport away from the connecting cilium toward the cell body or into the outer segment would require a plus end–directed motor such as kinesin-II. Previous work established that kinesin-II is required for the proper construction and maintenance of motile cilia in *Chlamydomonas, Tetrahymena*, and sea urchin, as well as cilia on mouse embryonic nodal cells, and immotile chemosensory cilia in *C. elegans* (for review see Marszalek and Goldstein, 2000). The defects we observe in KIF3A^{null}/KIF3A^{null} photoreceptor cells are

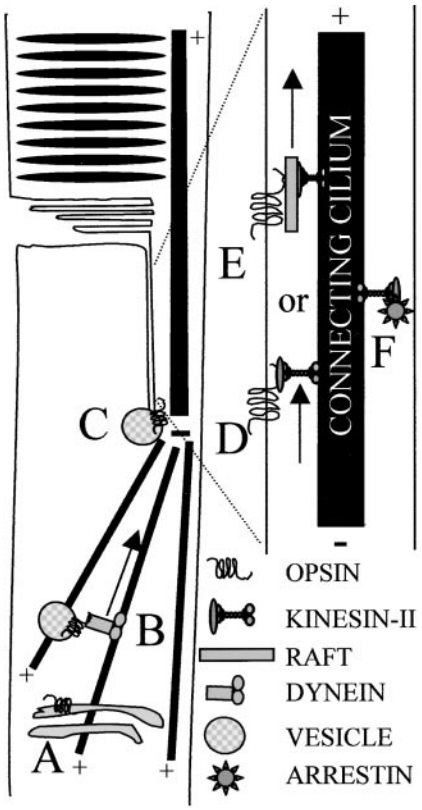

Figure 7. A Model for Opsin Transport to the Photoreceptor Outer Segment by Kinesin-II

(A) Opsin is processed in the Golgi apparatus and put into vesicles. (B) The carboxyl tail of opsin may interact with the Tctex-1 dynein light chain and is transported along microtubules to the basal body (Tai et al., 1999). (C) At the basal body the opsin-containing vesicle may fuse with the plasma membrane. Once in the plasma membrane, kinesin-II may interact directly with opsin (D) or through a raft complex (E) and be transported to the outer segment. (F) Arrestin may also be transported to the outer segment through the connecting cilium by kinesin-II.

most consistent with a function of kinesin-II in transport within the highly specialized immotile connecting cilium. Since the transport of several proteins to the synapse appeared to be unaltered in KIF3A^{null}/KIF3A^{null} photoreceptor cells, we conclude that transport of material from the inner segment to the synapse is less sensitive to loss of kinesin-II. Additionally, the structure of the Golgi apparatus in mutant photoreceptor cells appeared normal and aberrantly localized opsin was glycosylated, suggesting that opsin is processed normally through the Golgi apparatus in mutant cells. These data suggest that the primary function of kinesin-II in photoreceptors is not in protein glycosylation and processing as was reported in *Xenopus* XL177 and A6 cell lines (Le Bot et al., 1998). Taken together, these results support a role for kinesin-II in transport within the cilium of photoreceptor cells.

It is likely that kinesin-II is an essential motor needed for the transport of opsin to the outer segment for the following reasons. First, aberrant accumulation of opsin within the inner segment of KIF3A^{null}/KIF3A^{null} photoreceptor cells was the first and most common abnormality we observed, probably preceding misaccumulation of peripherin or activation of the apoptotic cell death pathway. Second, the opsin mislocalization defect we observed in KIF3A^{null}/KIF3A^{null} photoreceptors is similar to what has been reported for transgenic mice that express Q344ter mutant opsin in which opsin transport to the outer segment appears to be defective (Sung et al., 1994). In this context, it was recently reported that mutations in the tail domain of opsin might prevent it from interacting with tctex-1, a dynein light chain. Such mutants thus might interfere with the transport of mutant opsin by dynein to the connecting cilium (Tai et al., 1999). Third, the misaccumulation of opsin (Q344ter and P23H) and activation of the apoptotic pathway (P347S) that has been reported for opsin mutant mice is very similar to what we observed in KIF3A^{flox}/KIF3A^{null}; *cre*^{IRBP} neuroretinas, suggesting that the same set of general pathways may be disrupted in all of these mutants (Chang et al., 1993). The observation that the initial defect in opsin transport mutants in *Drosophila* is increased levels of opsin within the endoplasmic reticulum, eventually leading to the death of the cell is also consistent with this view (Colley et al., 1995).

Together, the data suggest that when the KIF3A protein level decreases to a point where opsin can not be efficiently transported to the outer segment, it "backs-up" within the inner segment. One speculation is that docking sites located around the basal body or connecting cilium become saturated when opsin is not transported properly to the outer segment. Since opsin is the most heavily trafficked cargo to the outer segment, back-up of opsin would result ultimately in the accumulation of many additional outer segment cargoes (e.g., peripherin) within the inner segment and therefore eventually block all transport to the outer segment (Figures 3A–3B).

An intriguing finding in this study is the colocalization of the cytosolic protein arrestin with mislocalized opsin in mutant inner segments. The simplest explanation for the arrestin mislocalization is that it is a cargo for kinesin-II. In fact, kinesin-II in *Drosophila* has been implicated in transporting the cytoplasmic protein choline acetyltransferase within axons, suggesting that kinesin-II is capable of transporting a subset of cytoplasmic proteins (Ray et al., 1999). However, an alternative explanation suggested by the colocalization of arrestin with mislocalized opsin is that arrestin may be interacting with the misplaced opsin. Since transducin binds to nonphosphorylated opsin, transducin would be expected to bind misplaced opsin if it is not phosphorylated, but transducin localization is completely normal in mutant photoreceptors. Perhaps mislocalized opsin within the inner segment is inadvertently activated and phosphorylated, thus acting as a sink for arrestin to bind. Interestingly, persistent binding of arrestin to phosphorylated opsin has been suggested as a contributory factor that leads to photoreceptor degeneration in retinitis pigmentosa (Li et al., 1995; Rim and Oprian, 1995) and thus might also be contributory to cell death in KIF3A mutant photoreceptors. However, these models are speculative and require further work to determine whether arrestin is a cargo of kinesin-II or its mislocalization is a secondary effect of opsin mislocalization.

The final stages of photoreceptor degeneration in KIF3A^{flox}/KIF3A^{null}; *cre*^{IRBP} mice are remarkably similar to the degeneration that is observed in all of the RP mutant mice strains that have been reported (e.g., *rd*/β-phosphodiesterase, *rds*/peripherin, and opsin mutants

Q334ter and P347S, but not P23H) (Ishiguro et al., 1987; Nir and Papermaster, 1989; Nir et al., 1989, 1990; Cantera et al., 1990; Olsson et al., 1992; Chang et al., 1993; Huang et al., 1993; Roof et al., 1994; Li et al., 1996). In these well-characterized mouse strains, opsin becomes aberrantly localized to the plasma membrane at late stages of photoreceptor degeneration around the time they undergo apoptotic cell death. Additionally, detachment of the photoreceptors from the retinal pigmented epithelial cells in wild-type animals can also result in the accumulation of peripherin and opsin throughout the photoreceptor cell, most likely a consequence of a general reduction in the rate of transport to the injured outer segment, until its attachment is repaired (Fariss et al., 1997).

A Model for the Opsin Transport Pathway

Previous work suggests that the final posttranslational modifications of opsin are made within the Golgi apparatus where opsin is packaged into vesicles for transport to the distal inner segment at the basal body region (Papermaster et al., 1985; Deretic and Papermaster, 1991) (Figure 7A). Once at the basal body, opsin-containing vesicles appear to fuse with the plasma membrane (Papermaster et al., 1985; Deretic and Papermaster, 1991; Deretic et al., 1996). The hypothesis that opsin is transported through the connecting cilium, and not via an extracellular route as suggested previously (Besharse and Wetzel, 1995), is supported by the observation that myosin VIIa mutant animals exhibit an increased opsin signal within the connecting cilium of mutant photoreceptors (Liu et al., 1999). Like kinesin-II, myosin VIIa is present in the connecting cilium (Liu et al., 1997), where it may perform an auxiliary, less critical role than kinesin-II in transport of opsin to the outer segment, since in mouse, myosin VIIa mutant photoreceptors do not undergo obvious degeneration. However, in humans, myosin VIIa might be more critical since mutations in myosin VIIa result in Usher syndrome 1B, which includes progressive photoreceptor cell death (Weil et al., 1995).

As opsin is transported through the connecting cilium, it might interact directly with kinesin-II or its KAP3 nonmotor subunit (Figure 7D) or indirectly through other protein complexes (Figure 7E). In both *C. elegans* and *Chlamydomonas*, the kinesin-II complex appears to interact with a large proteinaceous "raft" complex that is composed of 15 different protein subunits (Cole et al., 1998). A series of experiments established that in *Chlamydomonas* and *C. elegans*, the raft complex is transported from the cell body to the tip of the cilium by the plus end–directed kinesin-II, and returned to the cell body by the minus end–directed cytoplasmic dynein (Pazour et al., 1998, 1999; Signor et al., 1999). It is believed that the raft complex acts as a carrier or attachment structure for cargo transport, which cycles between the cell body and tip of the cilium by the action of kinesin-II and dynein. Interestingly, electron microscopy of *Chlamydomonas* flagella revealed that the plasma membrane that is adjacent to a raft is displaced inward against the raft (Kozminski et al., 1993; Cole et al., 1998). In addition, motility of glycoproteins within the flagellar membrane has been extensively studied and is believed to be a consequence of microtubule motors, consistent with the suggestion that the raft complex might associate with and transport integral membrane proteins such as opsin (Bloodgood, 1992) (Figures 7D and 7E).

However, biochemical attempts to isolate and identify the cargoes that interact with the raft complex have not been successful, perhaps because they are mediated by weak or transient interactions (Cole et al., 1998; Piperno et al., 1998). Our attempts to demonstrate direct binding of kinesin-II and opsin using coimmunoprecipitation and "GST pulldowns" with a GST-opsin fusion protein were unsuccessful, suggesting that if a direct interaction occurs between kinesin-II and opsin, it is of low affinity or requires cofactors to stabilize the interaction. A raft complex has not been reported in mammals, but the mouse homolog (NGD5) of the p52 subunit in *Chlamydomonas* and the osm-6 subunit of *C. elegans* has been identified (Cole et al., 1998). The presence of a raft subunit homolog in mouse suggests that raft complexes may also be used for transport along cilia in mammalian ciliated cells (Rosenbaum et al., 1999). However, further work is needed to determine whether the raft complex is utilized for transport along cilia in embryonic nodal and photoreceptor cells.

Relevance to Human Retinal Disease

Since complete loss of kinesin-II function in embryos (Nonaka et al., 1998; Marszalek et al., 1999; Takeda et al., 1999) results in embryonic lethality, it is unlikely that homozygous null mutations in kinesin-II subunits are a cause of human retinitis pigmentosa (RP). Reduction in the amount or efficiency of KIF3A protein, however, may decrease the efficiency of transport of new material through the connecting cilium needed to replace old material phagocytosed by the retinal pigmented epithelial (RPE) cells. Interestingly, moderately accelerated photoreceptor cell death has been reported to occur in mice that possess one deleted copy of rhodopsin (Humphries et al., 1997; Lem et al., 1999), suggesting that reduction in the amount of outer segment proteins is also generally deleterious and can lead to photoreceptor cell death. Based on our results, it will be important to determine whether any patients with hereditary RP have defects in components of the kinesin-II cilia transport pathway.

Experimental Procedures

Generation of the KIF3A Conditional Allele

The construction of the KIF3A targeting vector, introduction into R1 embryonic stem (ES) cells, and recombination to generate ES cells containing the KIF3A conditional allele (KIF3A^{flox}) was previously described (Chui et al., 1997; Marszalek et al., 1999). Four independent KIF3A^{flox} lines were established from sibling clones by backcrossing to the C57BL/6 inbred mouse strain. KIF3A mice used for analysis were a mixture of 129/SV/J and C57BL/6 inbred strains.

Generation of the IRBP-Cre Transgenic Animals

The *cre*^{IRBP} transgene vector was constructed by inserting the *cre* recombinase coding sequence into the pML177*mcs* vector, which contains the human growth hormone gene. The 1.3 kb fragment of the IRBP promoter was added to generate the IRBP-Cre recombinase transgene plasmid (p*cre*^{IRBP}). The *cre*^{IRBP} transgene DNA was introduced in CBA/Bl/6 F1 hybrid mouse oocytes by pronuclear injection. One mouse was identified that possessed the *cre*^{IRBP} transgene and this founder was backcrossed to C57BL/6 animals to establish the *cre*^{IRBP} transgenic line.

Genotyping and Quantification by PCR

The PCR primers used to identify the three KIF3A alleles were described in (Marszalek et al., 1999). The KIF3A^{flox} is ~130 bp larger than the KIF3A^{WT} allele because of the insertion of the loxP site. The presence or absence of the *cre*^{IRBP} transgene was determined using PCR with primers specific to the cre-recombinase coding sequence: cre-forward, CTGCATTACCGGTCGATGCA and cre-reverse, ACGT TCACCGGCATCAACGT (data not shown). Quantitative PCR was performed using 25 ng of neuroretina DNA that was purified as described (Marszalek et al., 1999). PCR fragments were separated on a 1.5% agarose gel and the gel image was captured and the bands quantified using a Stratagene Eagle Eye imaging system. To allow quantification of recombination frequency, we constructed a standard curve by mixing known amounts of KIF3A^{flox}/KIF3A^{WT} DNA with KIF3A^{WT}/KIF3A^{null} DNA, doing the PCR, running the gel and determining the band intensities. As Figure 2B shows, the PCR is very linear allowing for an accurate determination of recombination by the cre recombinase. For each KIF3A^{flox}/KIF3A^{WT}; *cre*^{IRBP} animal, the amount of conversion of the KIF3A^{flox} allele to KIF3A^{null} allele was determined by dividing the intensity of the band corresponding to the KIF3A^{null} allele by the sum of the band intensities of the KIF3A^{flox} and KIF3A^{null} alleles, then multiplying by 100 to obtain the percentage of KIF3A^{null} allele. The Student t test (two-tailed with two sample equal variance) was used to compare the distribution of cre-mediated recombination among animals of different ages.

Western Immunoblotting

Western immunoblotting of the neuroretina and brain from KIF3A^{WT}/KIF3A^{WT} and KIF3A^{flox}/KIF3A^{flox} was performed as described (Marszalek et al., 1999).

Processing of Tissue for Light and Electron Microscopy

Sacrificed animals were perfused with 1× PBS followed by fixation with 2% paraformaldehyde/2.5% glutaraldehyde/0.1 M Na-cacodylate for light and electron microscopy (EM). For immuno-EM, 1.5% glutaraldehyde was used instead of 2.5%. The eye was removed and placed in fixative for 10′, slit with a razor blade, fixed for an additional 15′, the anterior part of the eye and cornea were removed, and the remaining portion containing the neuroretina was returned to fixative at 4°C until processing for electron microscopy. Retinas were osmicated and then dehydrated with a graded series of ethanol, followed by propylene oxide, and finally embedded in epon for morphology at the EM level or embedded in LR white for immuno-EM.

For light microscopy, 0.8 μm sections were cut, mounted on slides, and then stained with toluidine blue. For EM, ultrathin sections were cut and mounted on grids before staining with uranyl acetate. Immunolabeling of grids was performed as described by (Liu et al., 1999).

Processing of Tissue and Immunofluorescence Analysis

For IF, eyes were processed as described in the previous section except that they were fixed using 4% paraformaldehyde in 0.1 M Sorenson's phosphate. Retinas were cryoprotected by a 2 hr incubation in 30% sucrose/PBS and then embedded in OCT compound.

Retinas were permeabilized and blocked with blocking reagent (0.1% Triton-X 100/1% BSA/1× PBS) for at least 1 hr. Antibodies were diluted in blocking reagent and added to the tissue on the slide for 2 hr at room temperature (RT). Slides were washed three times with 1× PBS for 10 min each. Secondary antibodies (Jackson Immunoresearch FITC, Texas red conjugated anti-mouse and/or anti-rabbit) were diluted (1:100) in blocking reagent and incubated for 1 hr at RT. Slides were washed three times for 15 min each and then mounted with vectashield (Vector Laboratories) and observed on a Bio-Rad MRC1000 confocal scanning microscope.

The following probes were used on retinas: (1:300) mAb B6–30 anti-opsin (Dr. Paul Hargrave), (1:500) anti-opsin (pAbs 01 and 99, Liu et al., 1999), (1:1000) pAb anti-peripherin/rds (Dr. Gabriel Travis), (1:75) mAb (A9C6) Arrestin (Dr. Larry Donoso), (1:100) pAb α-transducin (Dr. James Hurley), (1:50) mAb anti-SV2 (DSHB), (1:100) mAb anti-Cox I (Molecular Probes, Oregon), (1:500) pAb anti-calreticulin (Stressgen, Victoria, BC, Canada), mAb anti-giantin (Linstedt and Hauri, 1993), (1:1000) FITC conjugated Concanavalin A (Vector Laboratories).

Quantification of Cells in the Neuroretina

Quantification of the number of photoreceptors in the neuroretina was performed using light microscopy. The numbers of nuclei within a rectangle 140 μm wide were counted in three random areas of the outer nuclear layer, excluding the most peripheral 100 μm of the retina. The three numbers were then averaged to get a count for each retina. There was little variation among areas sampled within every retina examined.

TUNEL Staining for Apoptosis Detection

Detection of apoptotic cells within the retina was performed using the fluoroscein cell death kit (cat # 1,684,795) following the manufacturer's instructions. These retinas were then stained for the presence of opsin as described in the IF sections and observed on the confocal microscope.

Acknowledgments

We thank Dr. Paul Hargrave, Dr. Gabriel Travis, Dr. Larry Donoso, Dr. James Hurley, Dr. T. Linstedt, and the Developmental Studies Hybridoma Bank (DSHB—supported by NIH contract N01-HD-6-2915) for providing antibodies used in this study. We also thank members of the Goldstein, Williams, and Cleveland labs for constructive comments during the course of this work. This work was supported by grants from the NIH (EY07042 to D. S. W.) and the Foundation for Fighting Blindness (D. S. W.). J. R. M. was supported in part by an NIH predoctoral pharmacology training grant. L. S. B. G. is an Investigator of the Howard Hughes Medical Institute.

Received January 11, 2000; revised June 6, 2000.

References

Beech, P.L., Pagh-Roehl, K., Noda, Y., Hirokawa, N., Burnside, B., and Rosenbaum, J.L. (1996). Localization of kinesin superfamily proteins to the connecting cilium of fish photoreceptors. J. Cell Sci. *109*, 889–897.

Besharse, J.C., and Wetzel, M.G. (1995). Immunocytochemical localization of opsin in rod photoreceptors during periods of rapid disc assembly. J. Neurocytol. *24*, 371–388.

Bloodgood, R.A. (1992). Directed movements of ciliary and flagellar membrane components: a review. Biol. Cell *76*, 291–301.

Bobola, N., Hirsch, E., Albini, A., Altruda, F., Noonan, D., and Ravazzolo, R. (1995). A single cis-acting element in a short promoter segment of the gene encoding the interphotoreceptor retinoid-binding protein confers tissue-specific expression. J. Biol. Chem. *270*, 1289–1294.

Cantera, R., von Schantz, M., Chader, G.J., Ehinger, B., Sanyal, S., and van Veen, T. (1990). Postnatal development of photoreceptor-specific proteins in mice with hereditary retinal degeneration. An immunocytochemical study. Exp. Biol. *48*, 305–312.

Chang, G.Q., Hao, Y., and Wong, F. (1993). Apoptosis: final common pathway of photoreceptor death in rd, rds, and rhodopsin mutant mice. Neuron *11*, 595–605.

Chui, D., Oh-Eda, M., Liao, Y.F., Panneerselvam, K., Lal, A., Marek, K.W., Freeze, H.H., Moremen, K.W., Fukuda, M.N., and Marth, J.D. (1997). Alpha-mannosidase-II deficiency results in dyserythropoiesis and unveils an alternate pathway in oligosaccharide biosynthesis. Cell *90*, 157–167.

Cole, D.G., Chinn, S.W., Wedaman, K.P., Hall, K., Vuong, T., and Scholey, J.M. (1993). Novel heterotrimeric kinesin-related protein purified from sea urchin eggs. Nature *366*, 268–270.

Cole, D.G., Diener, D.R., Himelblau, A.L., Beech, P.L., Fuster, J.C., and Rosenbaum, J.L. (1998). Chlamydomonas kinesin-II-dependent intraflagellar transport (IFT): IFT particles contain proteins required for ciliary assembly in Caenorhabditis elegans sensory neurons. J. Cell Biol. *141*, 993–1008.

Colley, N.J., Cassill, J.A., Baker, E.K., and Zuker, C.S. (1995). Defective intracellular transport is the molecular basis of rhodopsin-dependent dominant retinal degeneration. Proc. Natl. Acad. Sci. USA *92*, 3070–3074.

Deretic, D., and Papermaster, D.S. (1991). Polarized sorting of rhodopsin on post-Golgi membranes in frog retinal photoreceptor cells. J. Cell Biol. *113*, 1281–1293.

Deretic, D., Puleo-Scheppke, B., and Trippe, C. (1996). Cytoplasmic domain of rhodopsin is essential for post-Golgi vesicle formation in a retinal cell-free system. J. Biol. Chem. *271*, 2279–2286.

Fariss, R.N., Molday, R.S., Fisher, S.K., and Matsumoto, B. (1997). Evidence from normal and degenerating photoreceptors that two outer segment integral membrane proteins have separate transport pathways. J. Comp. Neurol. *387*, 148–156.

Huang, P.C., Gaitan, A.E., Hao, Y., Petters, R.M., and Wong, F. (1993). Cellular interactions implicated in the mechanism of photoreceptor degeneration in transgenic mice expressing a mutant rhodopsin gene. Proc. Natl. Acad. Sci. USA *90*, 8484–8488.

Humphries, M.M., Rancourt, D., Farrar, G.J., Kenna, P., Hazel, M., Bush, R.A., Sieving, P.A., Sheils, D.M., McNally, N., Creighton, P., et al. (1997). Retinopathy induced in mice by targeted disruption of the rhodopsin gene. Nat. Genet. *15*, 216–219.

Ishiguro, S., Fukuda, K., Kanno, C., and Mizuno, K. (1987). Accumulation of immunoreactive opsin on plasma membranes in degenerating rod cells of rd/rd mutant mice. Cell Struct. Funct. *12*, 141–155.

Jeon, C.J., Strettoi, E., and Masland, R.H. (1998). The major cell populations of the mouse retina. J. Neurosci. *18*, 8936–8946.

Kozminski, K.G., Johnson, K.A., Forscher, P., and Rosenbaum, J.L. (1993). A motility in the eukaryotic flagellum unrelated to flagellar beating. Proc. Natl. Acad. Sci. USA *90*, 5519–5523.

Kozminski, K.G., Beech, P.L., and Rosenbaum, J.L. (1995). The Chlamydomonas kinesin-like protein FLA10 is involved in motility associated with the flagellar membrane. J. Cell Biol. *131*, 1517–1527.

Le Bot, N., Antony, C., White, J., Karsenti, E., and Vernos, I. (1998). Role of xklp3, a subunit of the Xenopus kinesin II heterotrimeric complex, in membrane transport between the endoplasmic reticulum and the Golgi apparatus. J. Cell Biol. *143*, 1559–1573.

Lem, J., Krasnoperova, N.V., Calvert, P.D., Kosaras, B., Cameron, D.A., Nicolo, M., Makino, C.L., and Sidman, R.L. (1999). Morphological, physiological, and biochemical changes in rhodopsin knockout mice. Proc. Natl. Acad. Sci. USA *96*, 736–741.

Li, T., Franson, W.K., Gordon, J.W., Berson, E.L., and Dryja, T.P. (1995). Constitutive activation of phototransduction by K296E opsin is not a cause of photoreceptor degeneration. Proc. Natl. Acad. Sci. USA *92*, 3551–3555.

Li, T., Snyder, W.K., Olsson, J.E., and Dryja, T.P. (1996). Transgenic mice carrying the dominant rhodopsin mutation P347S: evidence for defective vectorial transport of rhodopsin to the outer segments. Proc. Natl. Acad. Sci. USA *93*, 14176–14181.

Linstedt, A.D., and Hauri, H.P. (1993). Giantin, a novel conserved Golgi membrane protein containing a cytoplasmic domain of at least 350 kDa. Mol. Biol. Cell *4*, 679–693.

Liu, X., Vansant, G., Udovichenko, I.P., Wolfrum, U., and Williams, D.S. (1997). Myosin VIIa, the product of the Usher 1B syndrome gene, is concentrated in the connecting cilia of photoreceptor cells. Cell Motil. Cytoskeleton *37*, 240–252.

Liu, X., Udovichenko, I.P., Brown, S.D., Steel, K.P., and Williams, D.S. (1999). Myosin VIIa participates in opsin transport through the photoreceptor cilium. J. Neurosci. *19*, 6267–6274.

Marszalek, J.R., and Goldstein, L.S. (2000). Understanding the functions of kinesin-II. Biochim. Biophys. Acta *1496*, 142–150.

Marszalek, J.R., Ruiz-Lozano, P., Roberts, E., Chien, K.R., and Goldstein, L.S. (1999). Situs inversus and embryonic ciliary morphogenesis defects in mouse mutants lacking the KIF3A subunit of kinesin-II. Proc. Natl. Acad. Sci. USA *96*, 5043–5048.

Marth, J.D. (1996). Complexity in O-linked oligosaccharide biosynthesis engendered by multiple polypeptide N-acetylgalactosaminyltransferases. Glycobiology *6*, 701–705.

Muresan, V., Bendala-Tufanisco, E., Hollander, B.A., and Besharse, J.C. (1997). Evidence for kinesin-related proteins associated with the axoneme of retinal photoreceptors. Exp. Eye Res. *64*, 895–903.

Nir, I., and Papermaster, D.S. (1989). Immunocytochemical localization of opsin in degenerating photoreceptors of RCS rats and rd and rds mice. Prog. Clin. Biol. Res. *314*, 251–264.

Nir, I., Agarwal, N., Sagie, G., and Papermaster, D.S. (1989). Opsin distribution and synthesis in degenerating photoreceptors of rd mutant mice. Exp. Eye Res. *49*, 403–421.

Nir, I., Agarwal, N., and Papermaster, D.S. (1990). Opsin gene expression during early and late phases of retinal degeneration in rds mice. Exp. Eye Res. *51*, 257–267.

Nonaka, S., Tanaka, Y., Okada, Y., Takeda, S., Harada, A., Kanai, Y., Kido, M., and Hirokawa, N. (1998). Randomization of left-right asymmetry due to loss of nodal cilia generating leftward flow of extraembryonic fluid in mice lacking KIF3B motor protein. Cell *95*, 829–837.

Olsson, J.E., Gordon, J.W., Pawlyk, B.S., Roof, D., Hayes, A., Molday, R.S., Mukai, S., Cowley, G.S., Berson, E.L., and Dryja, T.P. (1992). Transgenic mice with a rhodopsin mutation (Pro23His): a mouse model of autosomal dominant retinitis pigmentosa. Neuron *9*, 815–830.

Papermaster, D.S., Schneider, B.G., and Besharse, J.C. (1985). Vesicular transport of newly synthesized opsin from the Golgi apparatus toward the rod outer segment. Ultrastructural immunocytochemical and autoradiographic evidence in Xenopus retinas. Invest. Ophthalmol. Vis. Sci. *26*, 1386–1404.

Pazour, G.J., Wilkerson, C.G., and Witman, G.B. (1998). A dynein light chain is essential for the retrograde particle movement of intraflagellar transport (IFT). J. Cell Biol. *141*, 979–992.

Pazour, G.J., Dickert, B.L., and Witman, G.B. (1999). The DHC1b (DHC2) isoform of cytoplasmic dynein is required for flagellar assembly. J. Cell Biol. *144*, 473–481.

Piperno, G., and Mead, K. (1997). Transport of a novel complex in the cytoplasmic matrix of Chlamydomonas flagella. Proc. Natl. Acad. Sci. USA *94*, 4457–4462.

Piperno, G., Siuda, E., Henderson, S., Segil, M., Vaananen, H., and Sassaroli, M. (1998). Distinct mutants of retrograde intraflagellar transport (IFT) share similar morphological and molecular defects. J. Cell Biol. *143*, 1591–1601.

Ray, K., Perez, S.E., Yang, Z., Xu, J., Ritchings, B.W., Steller, H., and Goldstein, L.S. (1999). Kinesin-II is required for axonal transport of choline acetyltransferase in Drosophila. J. Cell Biol. *147*, 507–518.

Rim, J., and Oprian, D.D. (1995). Constitutive activation of opsin: interaction of mutants with rhodopsin kinase and arrestin. Biochemistry *34*, 11938–11945.

Roof, D.J., Adamian, M., and Hayes, A. (1994). Rhodopsin accumulation at abnormal sites in retinas of mice with a human P23H rhodopsin transgene. Invest. Ophthalmol. Vis. Sci. *35*, 4049–4062.

Rosenbaum, J.L., Cole, D.G., and Diener, D.R. (1999). Intraflagellar transport: the eyes have it. J. Cell Biol. *144*, 385–388.

Signor, D., Wedaman, K.P., Orozco, J.T., Dwyer, N.D., Bargmann, C.I., Rose, L.S., and Scholey, J.M. (1999). Role of a class DHC1b dynein in retrograde transport of IFT motors and IFT raft particles along cilia, but not dendrites, in chemosensory neurons of living caenorhabditis elegans. J. Cell Biol. *147*, 519–530.

Sung, C.H., Makino, C., Baylor, D., and Nathans, J. (1994). A rhodopsin gene mutation responsible for autosomal dominant retinitis pigmentosa results in a protein that is defective in localization to the photoreceptor outer segment. J. Neurosci. *14*, 5818–5833.

Tai, A.W., Chuang, J.Z., Bode, C., Wolfrum, U., and Sung, C.H. (1999). Rhodopsin's carboxy-terminal cytoplasmic tail acts as a membrane receptor for cytoplasmic dynein by binding to the dynein light chain Tctex-1. Cell *97*, 877–887.

Takeda, S., Yonekawa, Y., Tanaka, Y., Okada, Y., Nonaka, S., and Hirokawa, N. (1999). Left-right asymmetry and kinesin superfamily protein KIF3A: new insights in determination of laterality and mesoderm induction by kif3A$^{-/-}$ mice analysis. J. Cell Biol. *145*, 825–836.

Takeda, S., Yamazaki, H., Seog, D.H., Kanai, Y., Terada, S., and Hirokawa, N. (2000). Kinesin superfamily protein 3 (KIF3) motor transports fodrin-associating vesicles important for neurite building. J. Cell Biol. *148*, 1255–1266.

Troutt, L.L., and Burnside, B. (1988). Microtubule polarity and distribution in teleost photoreceptors. J. Neurosci. *8*, 2371–2380.

Weil, D., Blanchard, S., Kaplan, J., Guilford, P., Gibson, F., Walsh, J., Mburu, P., Varela, A., Levilliers, J., Weston, M.D., et al. (1995). Defective myosin VIIA gene responsible for Usher syndrome type 1B. Nature *374*, 60–61.

Whitehead, J.L., Wang, S.Y., Bost-Usinger, L., Hoang, E., Frazer, K.A., and Burnside, B. (1999). Photoreceptor localization of the KIF3A and KIF3B subunits of the heterotrimeric microtubule motor kinesin II in vertebrate retina. Exp. Eye Res. *69*, 491–503.